

REVISED VERTICAL WIND MODEL  
(Added for Earth-GRAM 2007 Version 1.2 and  
Updated For Earth-GRAM 2010)

F. W. Leslie and C.G. Justus  
December, 2008

Background and Overview

A small-scale vertical wind perturbation model has been part of the Global Reference Atmospheric Model (GRAM) since its 1995 release (Justus et al., 1995). Height-dependent standard deviations of vertical winds were taken from Justus et al. (1990), which is included as a Portable Data Format (pdf) report on the GRAM distribution Compact Disk (CD). This vertical wind model continued in GRAM through the 1999 release (Justus and Johnson, 1999) and Version 1.1 of the 2007 release.

Recent strong interest in Orion parachute landing simulations led to a recommendation at the June, 2008 Orion Landing Systems and Environments Technical Interchange Meeting, held at Marshall Space Flight Center (MSFC), that GRAM's vertical wind model be "modified to pick the vertical wind distribution as a function of horizontal wind, and as a function of whether the condition is land or water". An earlier version vertical wind model, designed to address these issues, was released (in October 2008) as Earth-GRAM 2007 Version 1.2. That model incorporated many features of boundary layer (BL) effects on vertical wind standard deviations. However, time-of-day effects were not addressed, atmospheric stability influence was represented in only an approximate fashion, and boundary layer depth was assumed to be a constant value of 1500 m. The revised vertical wind model discussed here, and being released as Earth-GRAM 2010, incorporates effects of these additional factors.

Model Description

This new model computes standard deviation for boundary-layer (BL) vertical wind ( $\sigma_w$ ) as a function of surface type (water or various land types), and "surface" horizontal wind (at 10 m height). Surface height (above Mean Sea Level, MSL) is interpolated from a 1-by-1 degree topographic data base in the new `atmosdat_E10.txt` file [or from Range Reference Atmosphere (RRA) surface altitude, if within the "zone of influence" of any RRA site]. BL depth (height of the top of the BL above the surface) is computed from a new time-of-day and stability-dependent model. Land cover type is given at 1 degree resolution from data in the new GRAM "atmosdat\_E10.txt" input file, and is taken from DeFries and Townshend (1994). Surface topography, at 1-by-1 degree resolution is from Gates and Nelson (1975).

Surface Type codes, given in the revised `atmosdat_E10.txt` file at 1-by-1 degree latitude-longitude resolution, are shown in Table 1. Surface roughness ( $z_0$ ) values assumed for each surface type were computed as the geometric mean value from a variety of sources. Values for  $z_0$  are also given in Table 1.

To account, in an approximate way, for influence of mountainous topography on  $z_0$ , values from Table 1 are increased linearly for surface altitudes above 1.5 km MSL, up to either a maximum surface height of 4.5 km, or to a maximum  $z_0$  of 3 m, whichever is appropriate.

Wind dependence is on "surface hourly average" wind speed, computed from wind components given by monthly mean wind at 10 m plus GRAM large-scale perturbed wind components at the "surface". Since GRAM large-scale wind perturbations change from profile-to-profile in a Monte-Carlo run, then surface wind speed changes from profile-to-profile.

Table 1 - Surface codes, given in atmosdat\_E10.txt, and associated z0 values.

Code	Land Cover Class	z0 (m)
0	water	u-dependent
1	broadleaf evergreen forest	0.6
2	coniferous evergreen forest and woodland	0.48
3	high latitude deciduous forest and woodland	0.42
4	tundra	0.0056
5	mixed coniferous forest and woodland	0.45
6	wooded grassland	0.12
7	grassland	0.046
8	bare ground	0.015
9	shrubs and bare ground	0.042
10	cultivated crops	0.065
11	broadleaf deciduous forest and woodland	0.45
12	data unavailable (re-assigned to Codes 4, 6, or 13, as appropriate)	-. -
13	ice	3.2E-4

As given above, surface roughness (z0) is based on the 1-by-1 degree surface type array (from the atmosdat\_E10.txt file), or for water uses

$$z0 = \alpha (u^*)^2 / g , \quad (1)$$

where  $\alpha$  is a constant,  $u^*$  is surface friction velocity, and  $g$  is acceleration of gravity (Donelan et al., 1993). For land surfaces,  $z0$  is taken from surface type in Table 1. For water, the simultaneous dependence of  $z0$  on  $u^*$  and  $u^*$  on  $z0$  is solved by a 4-step iteration process. There is also an option whereby the user may supply any desired  $z0$  value (between  $10^{-5}$  m and 3 m), to be used in place of these prescribed  $z0$  values.

Friction velocity is computed from the standard logarithmic "law of the wall" for neutral atmospheric stability, modified by a stability-dependent term ( $\psi$ )

$$u^* = 0.4 U10 / [ \ln(10/z0) - \psi(10/L) ] , \quad (2)$$

where  $U10$  is the "surface" wind speed (at 10 m height),  $L$  is the Monin-Obukhov scaling length (stability-dependent), and the BL wind profile function  $\psi$  is given by

$$\begin{aligned} \psi(10/L) = & -50 / L & \text{if } 1/L > 0 & \text{(stable)} \\ & 0.0 & \text{if } 1/L = 0 & \text{(neutral)} \\ & 1.0496 ( -10 / L )^{0.4591} & \text{if } 1/L < 0 & \text{(unstable).} \end{aligned} \quad (3)$$

The unstable formulation for  $\psi$  is from Hsu et al. (1999), and is a simplification of an often-used, but more complicated expression derived by Paulson (1970).

Inverse of the Monin-Obukhov length ( $1/L$ ) is calculated by a four-step process, based on information derived from Table 4-7, Table 4-8, and Figure 4-9 of Justus (1978):

(1) Compute a net radiation index (nri) that depends on solar elevation angle and time-of day (or night), where nri ranges from -3.5 (strong outgoing net radiation) to + 4.5 (strong incoming net radiation). See Justus (1978), Table 4-7.

(2) Compute a wind-speed factor  $F(U10)$  from empirically-derived functions

$$\begin{aligned} F(U10) = & (1 - U10 / 7.5) & \text{if } U10 < 6 \text{ m/s} \\ & 0.2 & \text{if } U10 = 6 \text{ m/s} \\ & 0.2 \text{ Exp}(12 - 2 U10 ) & \text{if } U10 > 6 \text{ m/s} \end{aligned} \quad (4)$$

(3) Compute a stability category  $S$  as a function of  $F(U10)$  and  $nri$  by

$$S = 4.229 - nri \times F \quad (5)$$

which is an empirical fit to Justus (1978) Table 4-7. Values of  $S$  are limited to 0.5 on the low side (most unstable) and 7.5 on the high side (most stable).

(4) Compute inverse Monin-Obukhov length versus stability category  $S$  and surface roughness length  $z_0$ , from

$$1/L = (1/4) \times (-0.2161 + 0.0511 S) \text{Log}_{10}(10/z_0) \quad (6)$$

which is an empirical fit to Figure 4-9 of Justus (1978). Steps (1) through (4) are similar to the methodology of Blackadar et al. (1974) for estimation of  $L$ .

Standard deviation of vertical wind,  $\sigma_w$ , is computed as a function of height above the surface ( $z$ ), and stability-dependent Monin-Obukhov length by relations:

$$\begin{aligned} \sigma_w &= 1.25 u^* (1 + 0.2 z/L) && \text{(stable; } 1/L > 0) \\ &1.25 u^* && \text{(neutral; } 1/L = 0) \\ &1.25 u^* (1 - 3 z/L)^{1/3} && \text{(unstable; } 1/L < 0) \end{aligned} \quad (7)$$

where the stable relation is from equation 1.33 of Kaimal and Finnigan (1994) and Pahlow et al. (2001), and the unstable relation is from equation (2), Page 161, of Panofsky and Dutton (1984), a relation which has been widely used to represent this factor for the unstable atmospheric surface layer (e.g. Kaimal and Finnigan, 1994; Blackadar, 1997; Johansson, et al., 2001; Dardier, et al., 2003). A variety of different formulations for  $\sigma_w$  in stable situations have been suggested, including a formula equivalent to the unstable relation in equation (7) [e.g. equation (8) and Table 1 of Mahrt et al., 2001]. However, a simple linear relationship for the stable case, such as given in equation (7), has been more widely used.

As shown by Panofsky (1978), Caughey and Palmer (1979), and Panofsky and Dutton (1984) [in discussion of their Figure 7.2], equation (7) is not expected to apply above about  $z = 0.1 h$ , where  $h$  is the boundary layer depth. Therefore, for stable and neutral cases,  $\sigma_w$  is limited to a value of  $3.75 u^*$ , while for unstable cases,  $\sigma_w$  is limited by the magnitude of the convective velocity  $w^*$ , to a value of  $\sigma_w < 0.62 w^*$ , where  $w^*$  is given by

$$w^* = u^* [-h / (0.4 L)]^{1/3} \quad (8)$$

(equation 4 of Panofsky, 1978), where  $h$  is the stability-dependent boundary layer depth. These limiting values account for transition from the surface layer to the convective layer ( $z/L < 0$ ) or to the stable boundary layer ( $z/L > 0$ ).

Boundary layer depth  $h$  is calculated from simplifications of methodologies given by Sugiyama and Nasstrom (1999), Batchvarova and Gryning (1991), and Seibert (2000). For stable-to-neutral cases, the methodology of Section 2.1 of Sugiyama and Nasstrom is used

$$h = 2 h_N / [1 + (1 + 4 h_N/L)^{1/2}] \quad (9)$$

except that their form for the neutral boundary layer depth ( $h_N$ ) is changed from

$$h_N = 0.2 u^* / f \quad (10)$$

to

$$h_N = u^* [ 80 / ( \omega^2 f ) ]^{1/3} \quad (11)$$

where  $f$  is the Coriolis parameter and  $\omega$  is the Brunt-Vaisala frequency.

For the unstable boundary layer, the time-dependent differential equation solution of Batchvarova and Gryning (1991), as expressed in Seibert (2000), is converted to an algebraic equation by assuming that  $dh/dt$  can be replaced by  $h f / 2$ . This operation yields an analytical equation for  $h$

$$h = h_N ( 1 - 0.1125 h / L )^{1/3} \quad (12)$$

whose solution can be found by iteration.

For time variation between sunrise (if applicable) and mid-day, a time-factor multiplier  $f(EI)$ , given by

$$f(EI) = 0.3 + 0.7 EI / EI_{md} \quad (13)$$

is applied, where  $EI$  is solar elevation at the current time and  $EI_{md}$  is mid-day solar elevation. This allows for time variation of boundary layer depth to be accounted for in an analytical fashion, rather than solution of a differential equation versus time.

Subject to the above-mentioned limiting values, the height-dependent equations (7) are used to compute sigma-w from the surface to the top of the boundary layer. As part of its original vertical wind model, GRAM file `atmosdat_E10.txt` also contains values of sigma-w at 5 km intervals (above MSL). Between the top of the BL and the next height for which sigma-w is available, linear interpolation is used to estimate sigma-w.

Calculation of the vertical wind perturbations in GRAM is not changed, only the methodology for computing standard deviation of vertical wind. Values of sigma-w are constrained to be 0.1 m/s or greater, since the perturbation calculation methodology does not work properly if sigma-w is zero. Calculation of mean vertical winds (typically a few cm/s or less) is still done by a Montgomery stream function approach, first implemented in GRAM-90 [Justus et al. (1991), Section 2.7].

### Example Model Output

Equations (2) through (8) can be used to compute standard deviation of vertical wind (sigma-w) as a function of height above the surface ( $z$ ), the surface roughness ( $z_0$ ), and the “surface, hourly average” wind speed ( $U10$ ). These have been implemented as the revised vertical wind model in Earth-GRAM 2010. In this model, values of  $U10$  are computed from wind components given by GRAM latitude-longitude-dependent monthly mean wind at 10 m height, plus GRAM large-scale perturbed wind components at the “surface”. For each randomly-selected wind profile in a Monte-Carlo simulation sequence, different large-scale wind perturbations are produced, so  $U10$  values used in the sigma-w model vary from profile to profile.

Figure 1 shows two sample profiles of horizontal wind speed from a 1000-profile Monte Carlo GRAM run for January near San Clemente (Lat=30N Lon=118.5W). The two smooth lines are profiles of “hourly mean speed” (computed from components of monthly mean winds plus large-scale perturbed winds). The two lines with detailed structure are profiles of total perturbed wind speed (monthly mean, plus large-scale and small-scale perturbations). These two sample profiles were the ones with largest and smallest values of hourly “surface” wind speed (out of the 1000 Monte Carlo profiles). Because of effects of surface wind speed ( $U10$ ) on  $u^*$ , as in equation (2), profiles of sigma-w corresponding to the horizontal wind speed profiles of Figure 1 would be considerably different from one another.

Table 2 provides January statistics for sigma-w, computed from 600+ profile Monte Carlo runs of Earth-GRAM 2010, at three different boundary layer altitudes above the surface ( $z$ ), and at a variety of sites. Sites examined include Edwards Air Force Base (low surface roughness,  $z_0=0.04$  m), Kennedy Space Center (KSC) land surface (moderate surface roughness,  $z_0=0.45$  m), KSC water surface, and ocean sites near San Clemente and in the North Atlantic (Lat 50N Lon 30W).

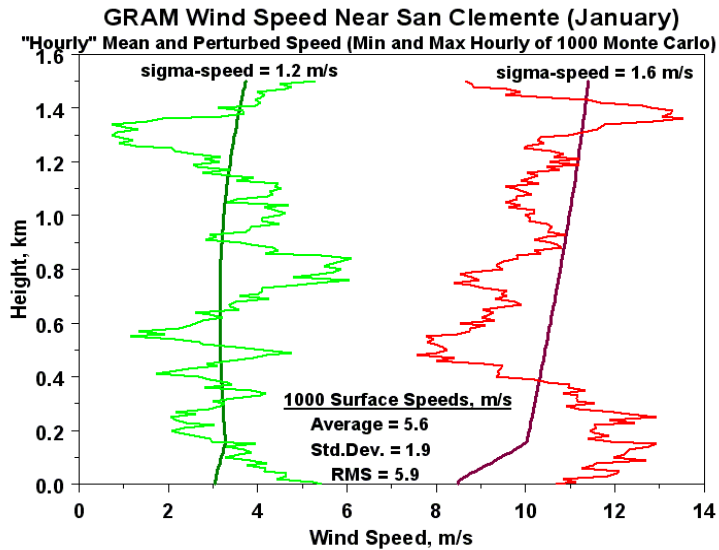


Figure 1 – Sample profiles of horizontal wind speed from a 1000-profile Monte-Carlo run for January, near San Clemente (Lat=30N, Lon=118.5W).

Table 2 – Sample output statistics for vertical wind standard deviation from GRAM-2010. KSC (land surface  $z_0 = 0.45$  m) is evaluated for February and June. Edwards AFB (land surface  $z_0 = 0.04$  m) and three water sites [KSC offshore, ocean near San Clemente, and North Atlantic ocean (Lat=50N Lon=30W)] are evaluated for February only.

	KSC Feb Land			KSC June Land		
Height (m)	10	100	1000	10	100	1000
Average	0.60	0.87	1.05	0.45	0.71	0.85
Std.Dev	0.25	0.38	0.49	0.21	0.42	0.54
Minimum	0.10	0.10	0.19	0.10	0.10	0.19
Maximum	1.29	1.75	2.38	1.10	1.92	2.69
	KSC Feb Water			Edwards AFB Feb		
Height (m)	10	100	1000	10	100	1000
Average	0.16	0.26	0.33	0.37	0.50	0.57
Std.Dev	0.06	0.11	0.10	0.20	0.25	0.24
Minimum	0.10	0.10	0.19	0.10	0.10	0.20
Maximum	0.36	0.57	0.57	0.85	1.11	1.23
	San Clemente Feb Water			N. Atlantic Ocean Feb		
Height (m)	10	100	1000	10	100	1000
Average	0.26	0.31	0.37	0.59	0.61	0.63
Std.Dev	0.12	0.12	0.10	0.32	0.30	0.28
Minimum	0.10	0.10	0.19	0.10	0.10	0.19
Maximum	0.58	0.58	0.58	1.79	1.79	1.79

As expected from equation (7), average sigma-w in Table 2 increases with z at all sites. The increase in z0 from Edwards to KSC land surface produces a significant increase in sigma-w. Change from KSC land surface to KSC water surface, with resultant decrease in z0 [by equation (1)], causes a significant decrease in sigma-w. With similar statistics for “hourly” surface wind speed, KSC water results and San Clemente values are fairly similar. However, because of substantially higher surface wind speeds at the North Atlantic site, there is a substantial increase in sigma-w over values for KSC (water) or San Clemente. Distributions of GRAM-computed hourly surface wind speeds at the San Clemente and North Atlantic sites are illustrated in Figures 2 and 3. Effects of stability are illustrated by comparison of sigma-w values from KSC February with KSC June. Lighter winds (hence smaller  $u^*$  values) in June make both the average sigma-w and the range of variability of sigma-w at 10 m height smaller for June than for February. While the average sigma-w for June at KSC remains lower at all altitudes, effects of convection under more prevalent unstable conditions in June make the range of sigma-w larger in June than in February, at both 100m and 1000m altitudes.

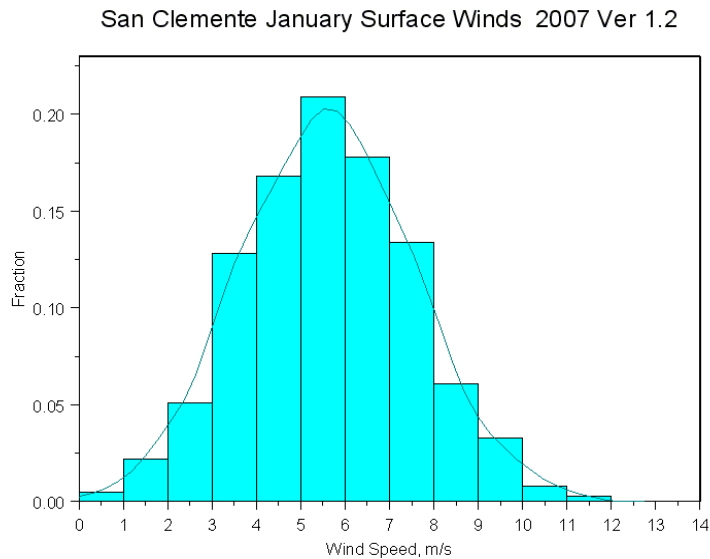


Figure 2 – Distribution of GRAM-computed January “hourly” surface wind speed at ocean site near San Clemente (Lat=30N Lon=118.5W).

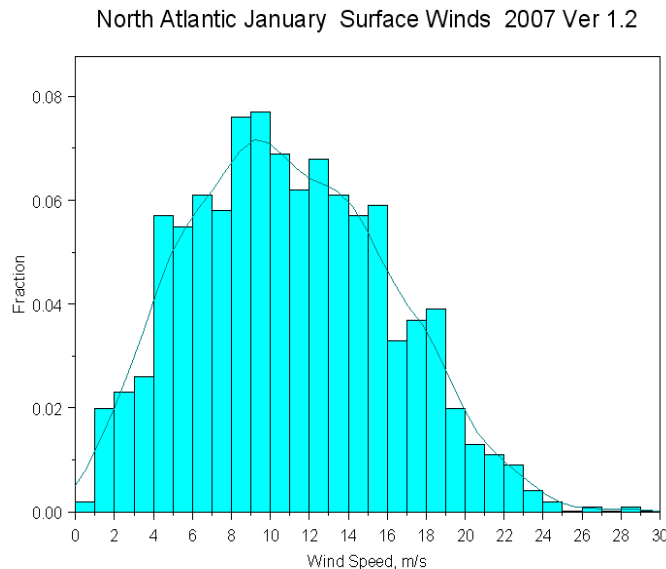


Figure 3 – Distribution of GRAM-computed January “hourly” surface wind speed at North Atlantic site (Lat=50N Lon=30W).

Figures 4 and 5 show examples of time-series calculations of BL height ( $h$ ) and vertical velocity standard deviation ( $\sigma_w$ ), for February. Because of variations in GRAM large-scale wind perturbations, boundary layer depth and  $\sigma_w$  are both seen to change from day to day, and to change regularly with time-of-day, as affected by stability and solar elevation angle effects.

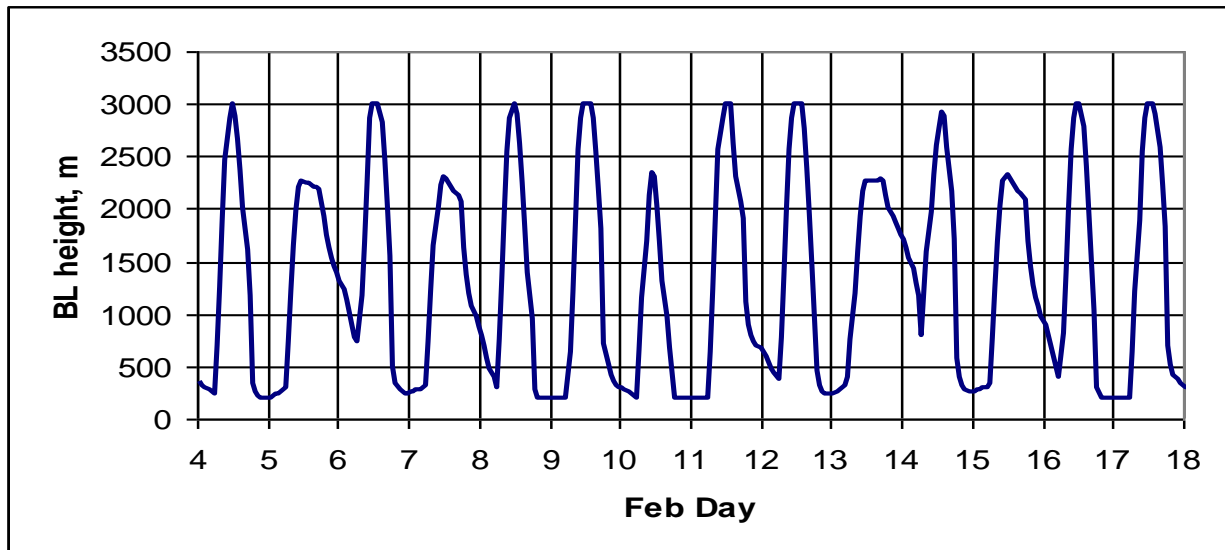


Figure 4 – GRAM-simulated time series for boundary layer depth ( $h$ ) for KSC February. Values of  $h$  are limited to between 200 m and 3000 m (see discussion above).

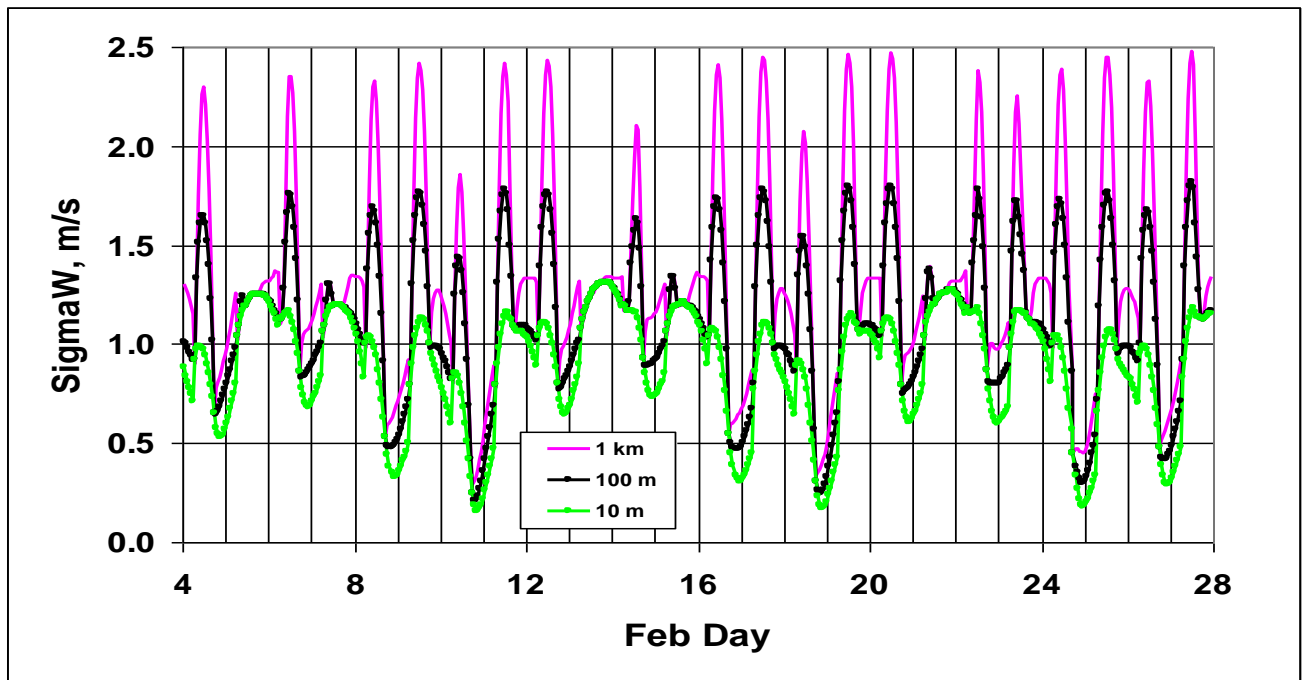


Figure 5 – GRAM-simulated time series of vertical wind standard deviation ( $\sigma_w$ ) for KSC February, at heights of 10, 100, and 1000 m.

## Model Validation

Vertical winds are roughly an order of magnitude smaller than horizontal winds. Vertical winds are correspondingly roughly an order of magnitude more difficult (and more expensive) to measure than horizontal winds. Consequently, availability of vertical wind measurements for model validation is fairly limited. For example, despite extensive meteorological instrumentation at KSC, vertical winds are not routinely measured (Frank Merceret, private communication). However, a limited amount of KSC vertical wind data, discussed below, provides some degree of model validation.

The surface roughness value ( $z_0 = 0.45$  m) used for KSC land surface results in Table 2, comes directly from the GRAM 1-by-1 degree global data base (discussed above). Nevertheless, this value is in good agreement with average  $z_0$  values at KSC determined from wind profile analysis by Fichtl (1968) and Blackadar et al. (1974), using the NASA 150-m meteorological tower.

In 1992 and 1993, the KSC Applied Meteorology Unit (2003) used a Doppler and Sound Detection-And-Ranging (SODAR) instrument (called a MiniSODAR™) to study horizontal and vertical winds near Space Launch Complex 37 (SLC-37) at KSC. They report (in their Figure 14) that vertical wind standard deviation during 17-30 June reached a diurnal peak of 0.57 m/s at about 1800 Hrs local time, at an altitude of 60 m. This MiniSODAR™ value is noticeably less than the maximum KSC sigma-w between 10 m and 100 m altitude from Table 2 for both February and June. Part of this discrepancy may be due to the limited sampling period (17-30 June) used by the Applied Meteorology Unit. It is also possible that the vertical winds are underestimated by the SODAR instrument, since the Applied Meteorology Unit report notes “an under-specification of vertical velocity variations by the phased array scanning sequence and the mathematical form of retrieval algorithms required for estimating peak wind speeds”, referred to elsewhere in the report as a problem with “under-sampling of the vertical wind velocity over the profiler beams”.

High-resolution tracking of balloon trajectories has also been used to estimate vertical winds near KSC. Rider and Armendariz (1970) measured sigma-w at KSC from high-resolution tracking of 37 wintertime and 10 summertime Jimsphere flights. At altitudes between 100 and 1200 meters, this study found that "Vertical wind components ranged from 10-25 cm/sec in a stable atmosphere to 55-100 cm/sec under unstable conditions, depending on wind speed". A maximum vertical wind of 100 cm/sec agrees fairly well with values at KSC (land surface) from Table 2. Record et al. (1970) measured sigma-w at KSC from high-resolution tracking of 10 overland and 5 overwater tetron flights. This study found (in their Table 2-3) that in four of the overland cases (40% of observations), 10-minute average sigma-w values exceeded 1 m/s, and that one of the five overwater cases had a 10-minute average sigma-w of 0.97 m/s, also in fairly good agreement with values from our Table 2.

Blackadar, et al. (1974) examined wind profiles observed from the KSC 150-m tower, and used observed mean speed at  $z = 18$  m (U18) and boundary layer (BL) theory to estimate surface roughness ( $z_0$ ), and surface friction velocity ( $u^*$ ). Although estimates of sigma-u and sigma-v are given, there are no direct measurements or estimates for sigma-w. However, Blackadar's Table 3 gives  $u^*$  values, from which approximate values for sigma-w can be calculated by  $\text{sigma-w} = \text{Factor}(z/L) \times u^*$  [e.g. as in equation 7, above]. Blackadar et al. give values of Richardson number ( $Ri$ ), from which values of  $z/L$  can be calculated, namely [from their equations (18) and (19)],

$$\begin{aligned} z/L &= Ri & (\text{unstable conditions}) \\ &= 5 Ri / (1 - 5 Ri) & (\text{stable conditions}). \end{aligned} \tag{14}$$

Table 3 gives a statistical summary computed from data given by Blackadar et al. Both estimated average sigma-w and maximum sigma-w from this table are somewhat larger than the GRAM-estimated values from Table 2, for heights up to 100 m.



Table 3 - Summary of KSC Vertical Wind Estimates (from data in Table 3 of Blackadar et. al., 1974)

	U18, m/s	z0, m	u*, m/s	Factor(z/L)	sigma-w (m/s) = Factor(z/L) x u*
Avg	4.88	0.46	0.67	1.58	1.04
StDev	2.47	0.17	0.28	0.32	0.41
Min	1.40	0.27	0.20	1.25	0.27
Max	11.70	0.79	1.47	2.79	2.36

-----

Note: Statistics from only those cases having estimated u\* values

The fact that estimates of sigma-w at KSC range from less than to greater than values given from GRAM estimates in Table 2 is taken as validation that the new GRAM vertical wind model is at least approximately correct, within the constraints and limitations of the present model. Some suggestions for further improvement in the model are given in the following sections, although, for reasons cited below, none of these are currently planned for implementation.

#### Notes for Earth-GRAM2010 Users

As mentioned above, the new vertical wind model makes use of surface roughness to compute sigma-w. These values are derived from a global database of land codes available in the input file "atmosdat\_E10.txt". While this input file has a resolution of 1° latitude by 1° longitude, this may not be of sufficient detail for some applications. For example, at a latitude of 28.62°N and longitude of 80.02°W which is about 57 km east of KSC launch complex 39 over the Atlantic Ocean, the database erroneously gives a land code of 5 (mixed coniferous forest and woodland) and a corresponding surface roughness of 0.45 m (see Table 1 above). Obviously the database does not spatially resolve details such as coastlines, etc. In order for the user to determine what land code (LC) and surface roughness (z0) was used by the model, these two parameters have been added to the special output file. So that the user may change the surface roughness used by the model, a new parameter z0in has been added to the NAMELIST input file. The user now has the option to supply a value of surface roughness between 10<sup>-5</sup> m and 3 m. To insure a water surface, z0in should be set to zero and the program will compute z0 from equations (1) and (2). Alternatively, setting z0in to a negative number signals the program to use the database mentioned above.

#### Suggestions for Further Model Development

As shown by Fichtl (1968) and Blackadar et al. (1974) surface roughness (z0), even at a relatively flat site such as KSC, can vary significantly with wind direction, due to variations in upwind characteristics (surface type, vegetation, terrain, etc.). There is no practical way in which GRAM can be modified to take into account all of these mesoscale and microscale effects. However, user input of desired value of z0 will continue to be a way to address these issues. In particular, it should be noted that the 1-by-1 degree lat-lon "box" in which KSC occurs, includes a large area that is water instead of land. Thus, if a GRAM users wants to simulate a water landing near KSC, the option of user-supplied z0 value should be used.

Using equation (2) the equation (7) accounts for effects of time-of-day, solar elevation, and atmospheric stability in the present model. However, the present model does not adequately address effects of solar and thermal radiation balance as influenced by cloud cover amount and cloud ceiling height. However, without extensive modifications (not currently planned), the influence of cloud cover and ceiling height on L [such as in Table 2 of Blackadar et al. (1974) or Tables 4-7 and 4-8 of Justus (1978)] cannot be explicitly incorporated into GRAM.

It has been shown that sigma-w can become quite large ( $\sim \pm 5$  m/s) under the influence of nearby topography (e.g. Furger et al., 2001). It is also well known that vertical wind in thunderclouds can be quite intense. Even fair-weather cumulus have been shown (Kollias, et al., 2001) to yield strong vertical winds ( $\sim 5$ -6 m/s). However, there is no practical way in which all of these mesoscale and microscale effects can be incorporated into GRAM, which is, by design, a global-scale model.

## References

Applied Meteorology Unit (2003): MiniSODAR™ Evaluation, NASA CR-2003-211192

Batchvarova, E. and Gryning, S. (1994): “An Applied Model for the Height of the Daytime Mixed Layer and the Entrainment Zone”, *Boundary-Layer Meteorology*, 71, 311–323.

Blackadar, A.K. (1997): “Turbulence and Diffusion in the Atmosphere”, Springer Publishing

Blackadar et al. (1974): “Investigation of the Turbulent Wind Field Below 500 Feet at the Eastern Test Range, Florida”, NASA CR-2438.

Caughey, S.J. and S.G. Palmer (1979): “Some aspects of turbulence structure through the depth of the convective boundary layer”, *Quarterly Journal of the Royal Meteorological Society*, 105, 811-827

Dardier, G. et al. (2003): “Constraining the inertial dissipation method using the vertical velocity variance”, *Journal of Geophysical Research*, 208, C3, 8063

DeFries, R. S. and J. R. G. Townshend (1994): "NDVI-derived land cover classification at a global scale.", *International Journal of Remote Sensing*, 15, 3567-3586.

Donelan, M.A. (1993): “On the Dependence of Sea Surface Roughness on Wave Development”, *Journal of Physical Oceanography*, 23, 2143-2149.

Fichtl, G.H. (1968): “Characteristics of Turbulence Observed at the NASA 150-m Meteorological Tower”, *Journal of Applied Meteorology*, 7, 838-844

Furger, M. et al. (2001): “Comparison of Horizontal and Vertical Scintillometer Crosswinds during Strong Foehn with Lidar and Aircraft Measurements”, *Journal of Atmospheric and Oceanic technology*, 18, 1975-1988

Gates, W.L., and A.B. Nelson (1975): "A New (Revised) Tabulation of the Scripps Topography on a 1deg Global Grid. Part I: Terrain Heights; Part II: Ocean Depths", Reports 1276,1277, Rand Corp., Santa Monica, Calif.

Hsu, S.A., B.W Blanchard, and Z. Yan (1999): “A Simplified Equation for Paulson’s  $\psi_m(Z/L)$  Formulation for Overwater Applications”, *Journal of Applied Meteorology*, 38, 623-625.

Johansson, C., et al. (2001): “Critical Test of the Validity of Monin–Obukhov Similarity during Convective Conditions”, *Journal of the Atmospheric Sciences*, 58, 1549-1566

Justus, C. G. (1978): “Winds and Wind System Performance”, Franklin Institute Press

- Justus, C. G. et al. (1990): “New Atmospheric Turbulence Model for Shuttle Applications”, NASA TM-4168.
- Justus, C.G. et al. (1991): “The NASA/MSFC Global Reference Atmospheric Model – 1990 Version (GRAM-90)”, NASA TM 4268
- Justus, C.G. et al. (1995): ”The NASA/MSFC Global Reference Atmospheric Model – 1995 Version (GRAM-95)”, NASA TM 4715
- Justus, C.G. and D.L. Johnson (1999): “The NASA/MSFC Global Reference Atmospheric Model – 1999 Version (GRAM-99)”, NASA/TM-1999-209630
- Kaimal, J.C., and J.J. Finnigan (1994): “Atmospheric Boundary Layer Flows”, Oxford University Press
- Kollias, P., et al. (2001): “Radar Observations of Updrafts, Downdrafts, and Turbulence in Fair-Weather Cumuli”, Journal of the Atmospheric Sciences, 58, 1750-1766
- Mahrt, L. et al. (2001): “Dependence of Turbulent and Mesoscale Velocity Variances on Scale and Stability”, Journal of Applied Meteorology, 40, 628-641
- Pahlow, M., M.B. Parlange and F. Porte-Agel (2001): “On Monin–Obukhov Similarity In The Stable Atmospheric Boundary Layer”, Boundary Layer Meteorology, 99, 225-248.
- Panofsky, H.A. (1978): “Matching in the Convective Planetary Boundary Layer”, Journal of the Atmospheric Sciences, 35, 272-276
- Panofsky, H.A. and J.A. Dutton (1984): “Atmospheric Turbulence”, John Wiley and Sons
- Paulson, C.A. (1970): “The mathematical representation of wind speed and temperature profiles in the unstable atmospheric surface layer”, Journal of Applied Meteorology , 9, 857–86.
- Record, F.A., et al. (1970): “Analysis of Lower Atmospheric Data for Diffusion Studies”, NASA CR-61327
- Rider, L.J. and M. Armendariz (1970): “Vertical Wind Component Estimates up to 1.2 km Above Ground”, Journal of Applied Meteorology, 9, 64-71
- Seibert, P. et al. (2000): “Review and intercomparison of operational methods for the determination of the mixing height”, Atmospheric Environment, 34, 1001-1027.
- Sugiyama, G. and J.S. Nasstrom (1999): “Methods for Determining the Height of the Atmospheric Boundary Layer, Lawrence Livermore Report, UCRL-ID-133200, February.